Supporting Information

Cobalt-based Multicomponent Oxygen Reduction Reaction Electrocatalysts Generated by Melamine Thermal Pyrolysis with High Performance in an Alkaline Hydrogen/Oxygen Micro-Fuel Cell

Haihong Zhong[a,b], Luis Alberto Estudillo-Wong[c], Yuan Gao[a], Yongjun Feng*[,a,d], Nicolas Alonso-Vante*[,b]

[a] *State Key Laboratory of Chemical Resource Engineering, Beijing Engineering Center for Hierarchical Catalysts, College of Chemistry, Beijing University of Chemical Technology, No. 15 Beisanhuan East Road, Beijing, 100029, China*

[b] *IC2MP, UMR-CNRS 7285, University of Poitiers, F-86022 Poitiers Cedex, France*

[c] *Departamento de Sociedad y Política Ambiental, CIIEMAD, Instituto Politécnico Nacional, Calle 30 de junio de 1520, Alcaldía GAM, C.P. 07340, CDMX, México.*

[d] *Anqing Research Institute, Beijing University of Chemical Technology, No. 8 Huanhu West Road, High-Tech district, Anqing city, Anhui, 24600, China.*

Corresponding Author

*E-mail addresses: yjfeng@mail.buct.edu.cn (Y.J. Feng); nicolas.alonso.vante@univ-poitiers.fr (N. Alonso-Vante)
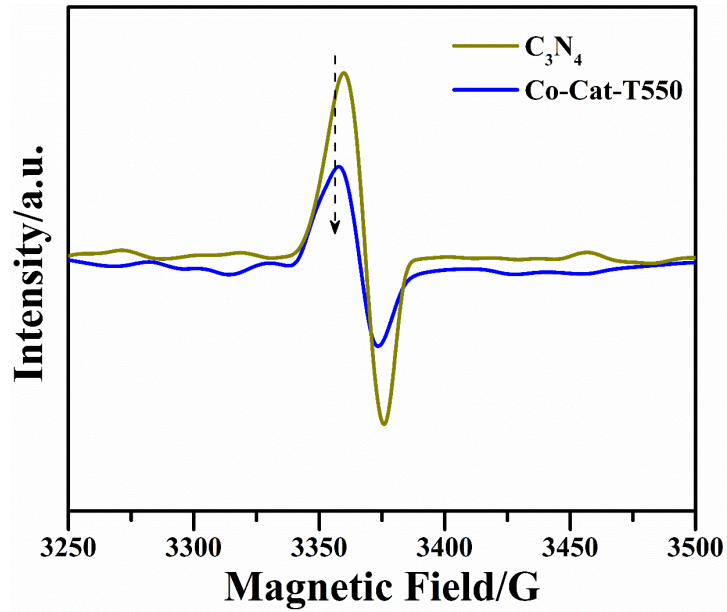
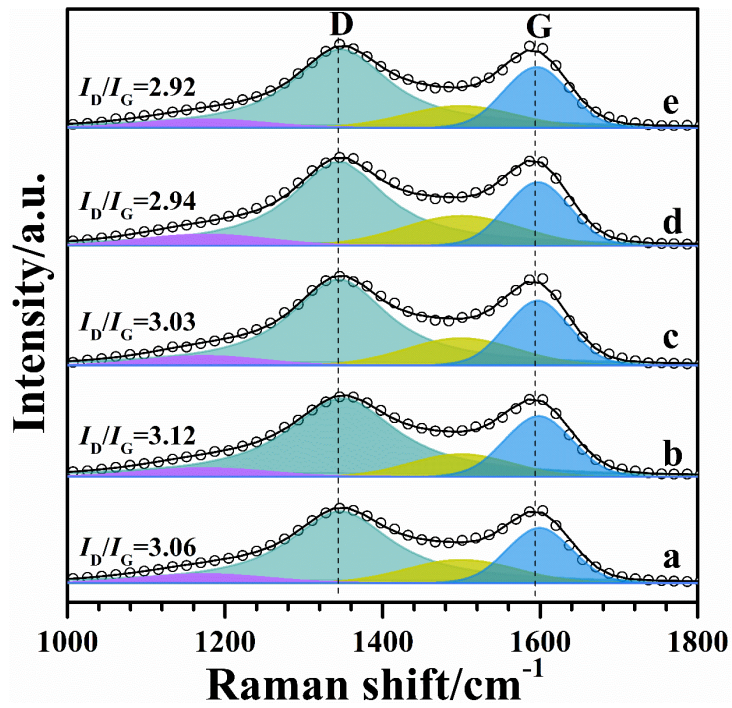**Figure S1.** EPR spectra of C_3N_4 and Co-Cat-T550.
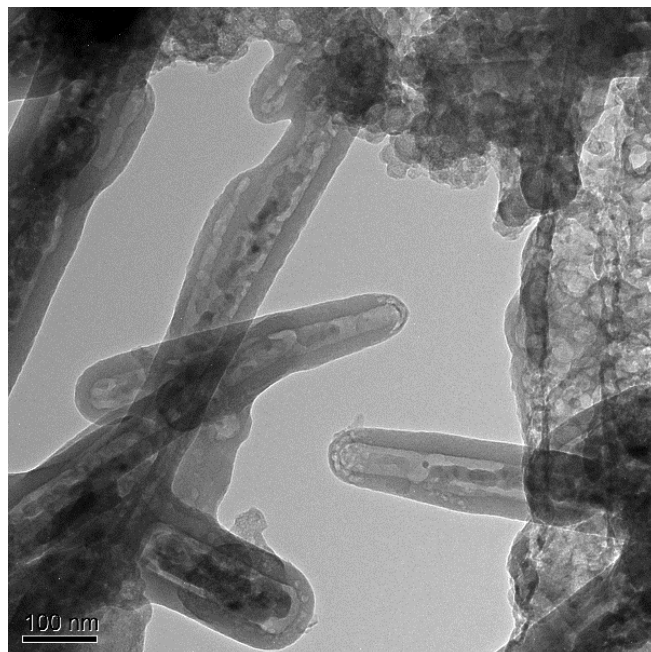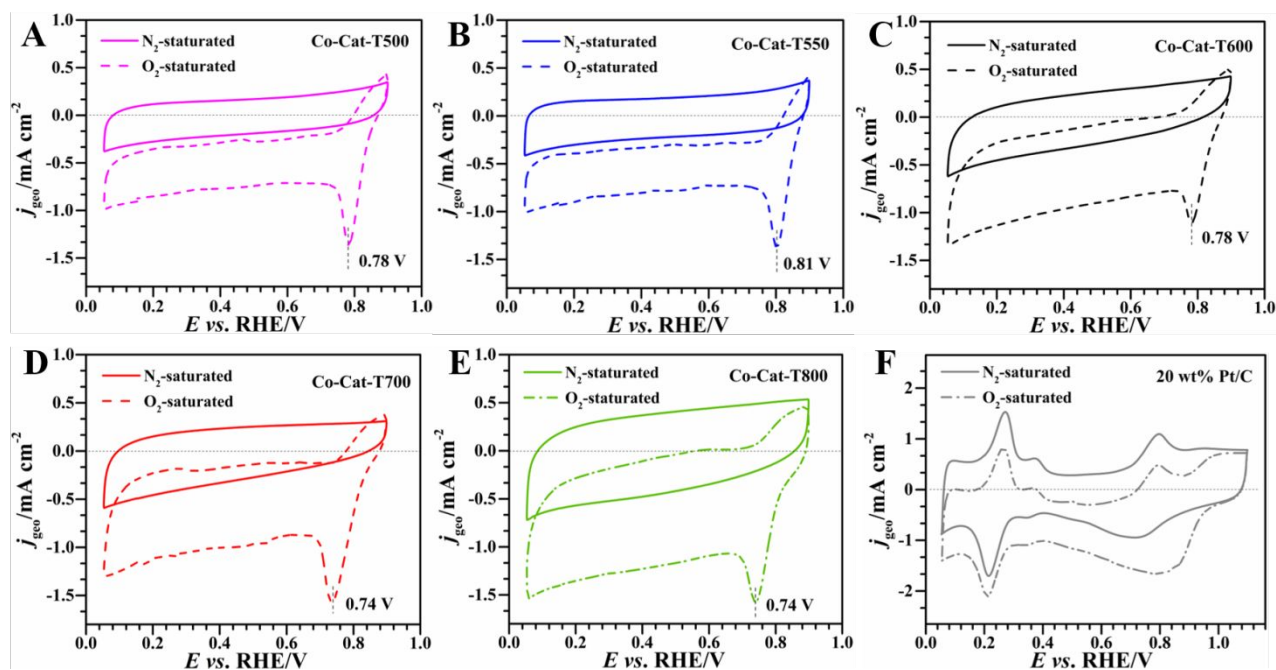

Figure S2. Raman spectra of all cobalt-based samples with labeled as: Co-Cat-T500 (a), T550 (b), T600 (c), T700 (d), T800 (e).
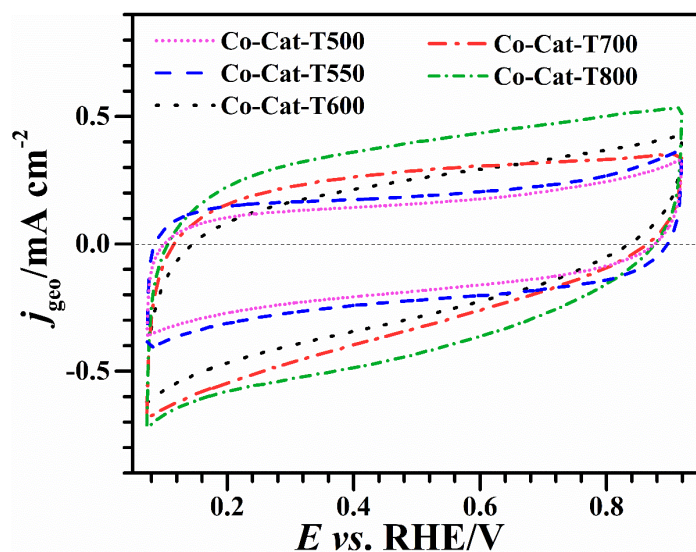
**Figure S3.** TEM image of Co-Cat-T550 sample.

Figure S4. (A-F) CV curves (ongoing positive scan) of the Co-Cat-T500, Co-Cat-T550, Co-Cat-T600, Co-Cat-T700, Co-Cat-T800 and 20 wt.% Pt/C catalysts in N_2 (solid line) and O_2-saturated (dash line) 0.1 M KOH

at a scan rate of 50 mV s^{-1}, respectively.

Figure S5. CV curves (ongoing positive scan) of the Co-Cat-T500, -T550, -T600, -T700, and -T800 in N$_2$-saturated 0.1 M KOH at a scan rate of 50 mV s^{-1}, respectively.
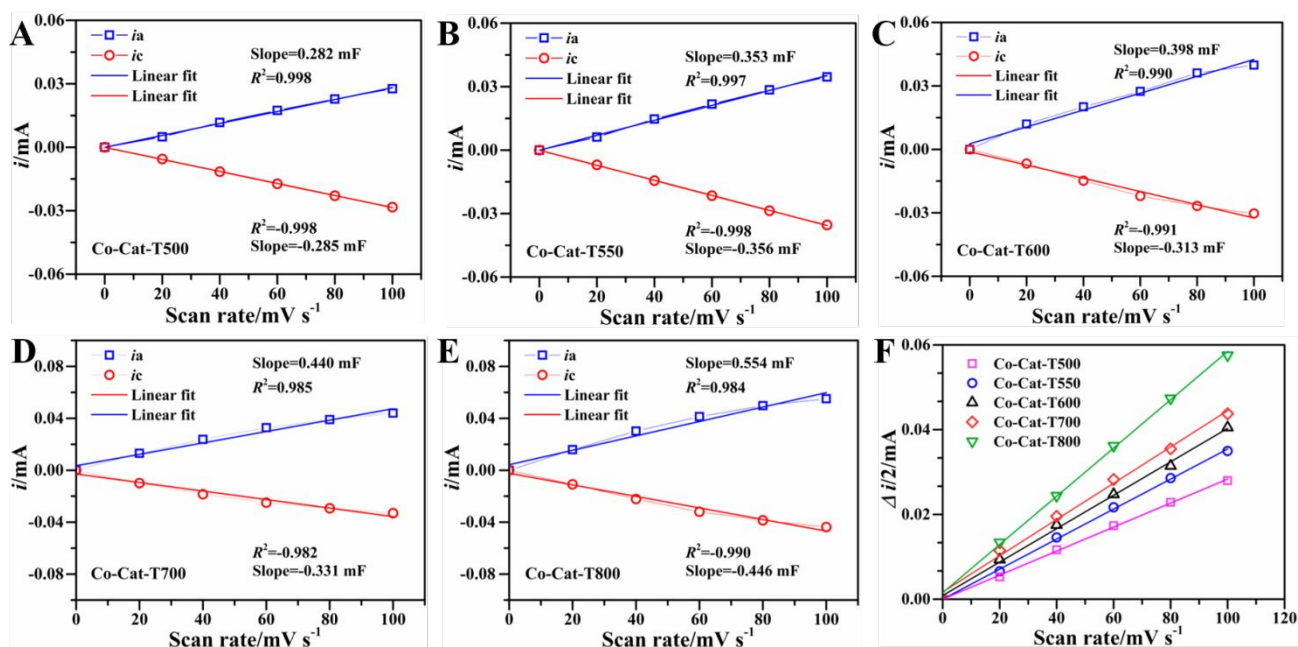
Figure S6. (A-E) ECSA measurement for all the samples at different scan rates from 20 to 100 mV s^{-1} in N$_2$-saturated 0.1 M KOH within a non-faradaic region of 0.30−0.40 V *vs*. RHE; (F) the capacitive currents of all the samples measured at 0.35 V *vs*. RHE were plotted as a function of scan rates from 20 mV s^{-1} to 100 mV s^{-1} at RT.
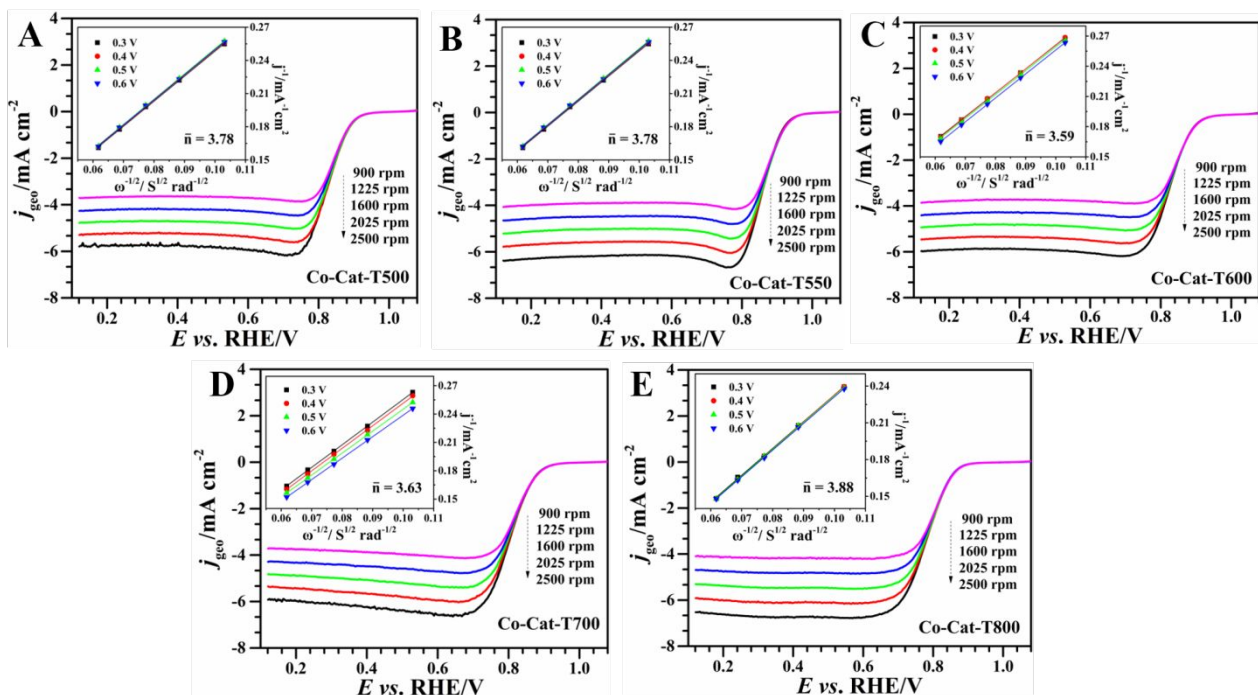
Figure S7. LSV curves of the Co-Cat-T500 (A), Co-Cat-T550 (B), Co-Cat-T600 (C), Co-Cat-T700 (D), and Co-Cat-T800 (E) c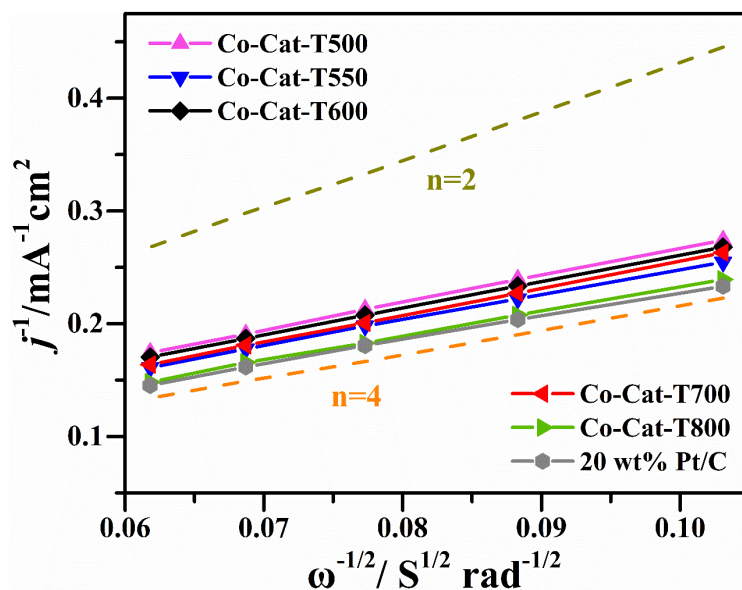atalysts in O_2-saturated 0.1 M KOH at a scan rate of 5 mV s^{-1} at different rotation speeds ranged from 2500 to 900 rpm, RT. Inset: the corresponding Koutecky-Levich plots derived from the LSV curves at different potentials.

Figure S8. The number of electrons transferred, n, per O_2 molecule calculated from K-L data.
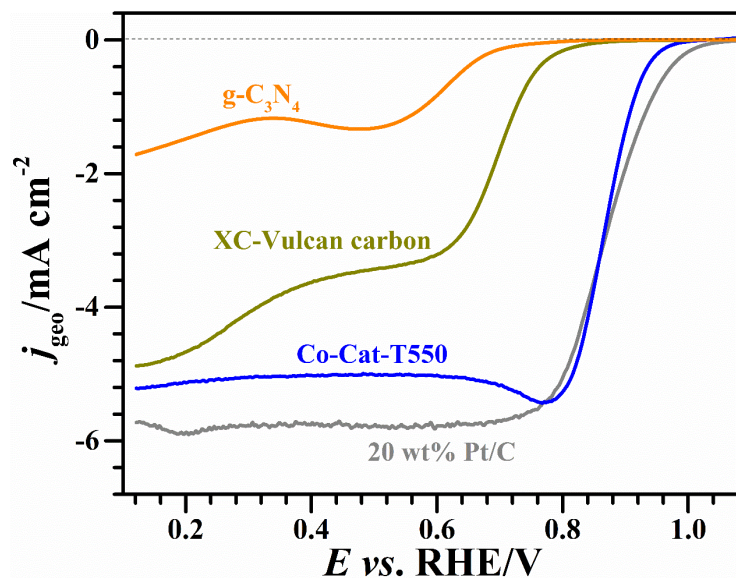
Figure S9. LSV curves (negative-going scan) of the pure g-C$_3$N$_4$, XC-Vulcan carbon, Co-Cat-T500, and commercial 20 wt.% Pt/C catalysts in O$_2$-saturated 0.1 M KOH at 1600 rpm, RT, at a scan rate of 5 mV s^{-1}.
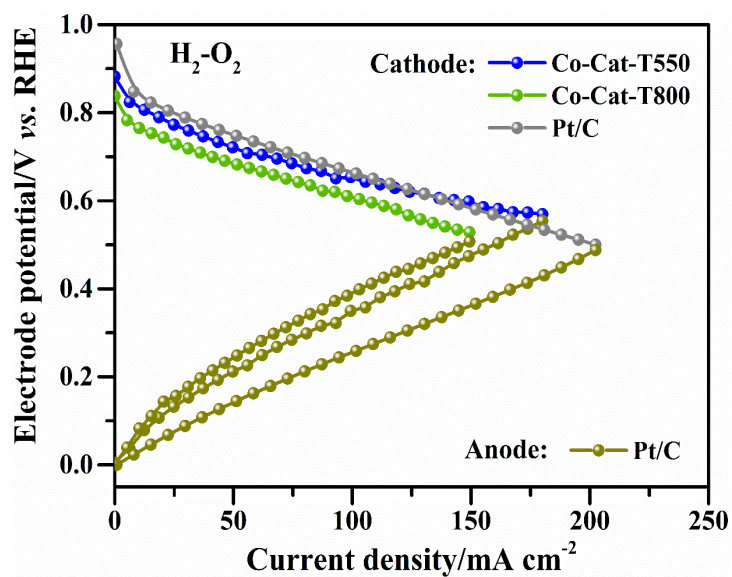
Figure S10. Current-potential curves, at RT, of the μLFFC with Co-Cat-T500, Co-Cat-T800 and Pt/C as cathode electrodes in 3 M KOH. 20 wt.% Pt/C was used as anode.

Table S1. XPS spectra analyses of N 1s signal (peak position and atomic percentage) for all heat-treated samples.

Catalysts	N					
	pyridinic-N (N1)	Co-N$_x$ (N2)	pyrrolic-N (N3)	graphitic-N (N4)	oxidized graphitic-N (N5)	Ratio of N4/N1
Co-Cat-T500	398.3 (65.7%)	399.5 (16.7%)	400.3 (11.9%)	--	(5.7%)	-
Co-Cat-T550	398.1 (65.8%)	399.3 (18.8%)	400.4 (11.3%)	-	(4.1%)	-
Co-Cat-T600	398.2 (47.7%)	399.1 (12.6%)	400.1 (2.7%)	401.0 (15.8%)	404.7 (21.2%)	0.33
Co-Cat-T700	398.1 (33.4%)	399.1 (13.7%)	400.2 (12.2%)	401.1 (21.9%)	404.9 (18.8%)	0.65
Co-Cat-T800	398.1 (29.1%)	399.1 (13.5%)	400.2 (11.2%)	401.4 (22.8%)	404.5 (23.4%)	0.78

Table S2. The onset potential (E_{onset}), cathodic potential of ORR peak ($E_{p,c}$ vs. RHE), half-wave potential ($E_{1/2}$ V vs. RHE), kinetic current density at 0.8 V ($j_{k,geo}$@0.8V/mA cm^{-2}), and Tafel slope (|b|/mV dec^{-1}) of all samples.

Catalysts	E_{onset}/V vs. RHE	$E_{p,c}$/V vs. RHE	$E_{1/2}$/V vs. RHE	$j_{k,geo}$@0.8V /mA cm^{-2}	Tafel slope |b| /mV dec^{-1}
Co-Cat-T500	0.93	0.78	0.83	3.33	60
Co-Cat-T550	0.96	0.81	0.86	11.24	52
Co-Cat-T600	0.94	0.78	0.83	3.21	64
Co-Cat-T700	0.92	0.74	0.81	1.73	67
Co-Cat-T800	0.90	0.74	0.78	0.83	62
20 wt.% Pt/C	1.01	0.80	0.86	10.58	66

Table S3. Comparison of ORR activities of Co-Cat-T (this work) with those reported for Co-based and commercial Pt/C catalysts in 0.1 M KOH solution.

Catalysts	E_{onset}/V vs. RHE	$E_{1/2}$/V vs. RHE	Tafel slope/ mV dec^{-1}	$E_{p, c}$/V vs. RHE	Ref.
Co-Cat-T550	0.96	0.86	52	0.81	This work
20% Pt/C	1.01	0.86	66	0.80	This work
NGT-Co$_{35}$V$_{65}$-45-900	0.92 (-0.05 mA cm^{-2})	0.81	66	~0.79	[1]
Co$_x$N/NHCS	-0.02 vs. SCE	-0.12 vs. SCE	89	-0.02 vs. SCE	[2]
Co/NC	0.98	0.87 V	102	0.83	[3]
Co–N/Co–O@N–C	0.93	N/A	51	N/A	[4]
Co-N-C/CoO$_x$-3	N/A	0.82	N/A	0.84	[5]
Co/NC	~0.90	0.83	N/A	N/A	[6]
Co-N@HCS	0.96	0.86	56	N/A	[7]
Co–N$_x$/C NRA	~0.97	0.88	66	0.87	[8]
CoCOF-Py-0.05rGO	0.84	0.77	N/A	0.75	[9]
CoN$_x$/NGA	0.93	0.83	66	0.78	[10]
Co-N-OMMC-0.6	N/A	0.83	N/A	0.78	[11]
CoO/N-rMdGO	0.89	082	57	N/A	[12]
CoO/rGO(N)	0.95	0.83	58	N/A	[13]

References:

1. Wang, Y.; Wang, L.; Tong, M.; Zhao, X.; Gao, Y.; Fu, H. Co-VN Encapsulated in Bamboo-like N-doped Carbon Nanotubes for Ultrahigh-stability of Oxygen Reduction Reaction. *Nanoscale* **2018,** *10* (9), 4311-4319.

2. Zhong, X.; Liu, L.; Jiang, Y.; Wang, X.; Wang, L.; Zhuang, G.; Li, X.; Mei, D.; Wang, J.-g.; Su, D. S. Synergistic Effect of Nitrogen in Cobalt Nitride and Nitrogen-doped Hollow Carbon Spheres for the Oxygen Reduction Reaction. *ChemCatChem* **2015,** *7* (12), 1826-1832.

3. Guan, B. Y.; Yu, L.; Lou, X. W. D. Formation of Single-holed Cobalt/N-doped Carbon Hollow Particles with Enhanced Electrocatalytic Activity toward Oxygen Reduction Reaction in Alkaline Media. *Adv. Sci.* **2017,** *4* (10), 1700247-1700252.

4. Lee, K. J.; Shin, D. Y.; Byeon, A.; Lim, A.; Jo, Y. S.; Begley, A.; Lim, D. H.; Sung, Y. E.; Park, H. S.; Chae,

K. H.; Nam, S. W.; Lee, K. Y.; Kim, J. Y. Hierarchical Cobalt-nitride and -Oxide co-doped Porous Carbon Nanostructures for Highly Efficient and Durable Bifunctional Oxygen Reaction Electrocatalysts. *Nanoscale* **2017,** *9* (41), 15846-15855.

5.   Xin, W.-L.; Lu, K.-K.; Shan, D. In Situ Doped $CoCO_3$/ZIF-67 Derived Co-N-C/CoO_x Catalysts for Oxygen Reduction Reaction. *Appl. Surf. Sci.* **2019,** *481*, 313-318.

6.   Aijaz, A.; Masa, J.; Rosler, C.; Xia, W.; Weide, P.; Botz, A. J.; Fischer, R. A.; Schuhmann, W.; Muhler, M. $Co@Co_3O_4$ Encapsulated in Carbon Nanotube-grafted Nitrogen-doped Carbon Polyhedra as An Advanced Bifunctional Oxygen Electrode. *Angew. Chem. Int. Ed. Engl.* **2016,** *55* (12), 4087-4091.

7.   Cai, S.; Meng, Z.; Tang, H.; Wang, Y.; Tsiakaras, P. 3D Co-N-doped Hollow Carbon Spheres as Excellent Bifunctional Electrocatalysts for Oxygen Reduction Reaction and Oxygen Evolution Reaction. *Appl. Catal. B: Environ.* **2017,** *217*, 477-484.

8.   Amiinu, I. S.; Liu, X.; Pu, Z.; Li, W.; Li, Q.; Zhang, J.; Tang, H.; Zhang, H.; Mu, S. From 3D ZIF Nanocrystals to Co-N_x/C Nanorod Array Electrocatalysts for ORR, OER, and Zn-Air Batteries. *Adv. Funct. Mater.* **2018,** *28* (5), 1704638-1704646.

9.   Zuo, Q.; Cheng, G.; Luo, W. A Reduced Graphene Oxide/covalent Cobalt Porphyrin Framework for Efficient Oxygen Reduction Reaction. *Dalton. Trans.* **2017,** *46* (29), 9344-9348.

10.   Zou, H.; Li, G.; Duan, L.; Kou, Z.; Wang, J. In Situ Coupled Amorphous Cobalt Nitride with Nitrogen-doped Graphene Aerogel as A Trifunctional Electrocatalyst towards Zn-air Battery deriven Full Water Splitting. *Appl. Catal. B: Environ.* **2019,** *259*, 118100-118110.

11.   Sun, T.; Xu, L.; Li, S.; Chai, W.; Huang, Y.; Yan, Y.; Chen, J. Cobalt-nitrogen-doped Ordered Macro-/mesoporous Carbon for Highly Efficient Oxygen Reduction Reaction. *Appl. Catal. B: Environ.* **2016,** *193*, 1-8.

12.   Mao, S. W., Z.; Huang, T.; Hou, Y.; Chen, J. High-performance Bi-functional Electrocatalysts of 3D Crumpled Graphene–cobalt Oxide Nanohybrids for Oxygen Reduction and Evolution Reactions. *Energy Environ. Sci.* **2014,** *7*, 609-609.

13.   He, Q.; Li, Q.; Khene, S.; Ren, X.; López-Suárez, F. E.; Lozano-Castelló, D.; Bueno-López, A.; Wu, G. High-loading Cobalt Oxide Coupled with Nitrogen-doped Graphene for Oxygen Reduction in Anion-exchange-membrane Alkaline Fuel Cells. *J. Phys. Chem. C* **2013,** *117* (17), 8697-8707.